Theor Chim Acta (1991) 81: 31–43

Theoretica Chimica Acta

Intermolecular vibronic coupling and energy transfer in a flat molecular aggregate*

Renato E. Varas[1] and Jorge Ricardo Letelier[2]

[1] Departamento de Matemáticas, and [2] Departamento de Química, Facultad de Ciencias Físicas y Matemáticas, Universidad de Chile, Casilla 2777, Santiago, Chile

Received May 30, 1990; received in revised form and accepted December 10, 1990

Summary. The migration of excitation within a small flat molecular aggregate composed of identical molecules is described using a Davidov-like model and a mechanism of excitation transfer of Förster type. We consider in this model the changes that take place in the equilibrium position of each molecule upon excitation and construct energy surfaces that describe "paths", that is, conditions for excitation localization and transfer that govern, in first-order, the motion of excitation within the aggregate.

Key words: Flat molecular aggregates – Migration of excitation – Energy surfaces – Excitation localization

1. Introduction

Since the pioneering work of Emerson and Arnold [1] on the physical account of the photosynthetic process, there has been renewed interest in the theoretical description of the physical delivery of excitation or energy from antenna or bulk chlorophyll molecules to a primary reaction center. In the Franck–Teller model [2], upon photon absorption, a molecule (or group of molecules) is excited and the excitation transferred to other molecules mainly through the interaction between transition dipole moments. The rate at which the excitation is transferred to a reaction center or "trap" has also been extensively studied [3, 9, 10].

In most of these theoretical descriptions of energy migration in aggregates of chlorophyll molecules, the phenomenon goes through a random walk process or through a localized excitation-diffusion process. In some of these models, the effect of molecular orientation has also been considered [4], in none of these models the role played by the molecular internal structure seems to have been considered.

The number of molecules in a chlorophyll aggregate usually amounts to several hundreds and therefore these models are appropriate for such a large scale. Our motivation, on the other hand, is the transfer of excitation in a small

* Presented in part at XVIII Jornadas Chilenas de Química, Santiago, 1989

scale where we have incorporated, with some detail, the internal structure of the participating molecules and the effect that coupling among them might have on the migration of excitation within the aggregate. It has been recently shown [8] that vibronic coupling plays an important role in the transfer and localization or "trapping" of excitation in a small three-dimensional molecular aggregate and that, whether a molecule will retain or forfeit the excitation will depend to a great extent on the magnitude of such coupling.

We have used and extended these ideas in the study of a small flat molecular aggregate and we show, in the present work, that there are energy surfaces arising from intermolecular vibronic coupling that might govern the dynamics of the phenomenon and, at least for small molecular clusters, where these effects become noticeable, there are steps or jumps, if we consider a random-walk model to describe the flow of excitation within the aggregate; these will show higher probability, because they lead to lower energy states, and therefore the energy or excitation might migrate within the aggregate through certain preferred or more probable "paths".

As the size of the aggregate increases, these effects in fact tend to vanish and on a large scale all steps become equally probable, which is the case of chlorophyll aggregates.

In the present work we will attempt to describe such "paths" in small flat molecular aggregates, consisting of closed-packed arrangements of 19 identical molecules, and describe the conditions for migration or trapping of energy in some specific centers of this cluster.

2. Formalism

In this formalism we assume that energy migrates within the molecular aggregate following an excitation transfer mechanism, between adjacent molecules, similar to that proposed by Förster in his study of excitation transfer between dimers [6]. We describe then the many-particle excited state within the framework of the delocalized electronic state theory of molecular excitons [7] and obtain the exciton states following a variational procedure.

In the present approach, we take into account the changes that occur in the internal structure of the individual molecules upon excitation transfer through the alteration of the whole-molecule equilibrium position, which in turn can be described by a single coordinate Q_i. There is no loss of generality in doing this because such description can always be done and Q_i not necessarily has to be a normal coordinate. For instance, we might look into the changes that take place in bond lengths in a totally symmetric vibration such as the molecular "breathing motion". In this coordinate there will be a ground-state equilibrium position Q_0 and an excited-state equilibrium position Q_0^* which have the same value for all molecules.

The Hamiltonian for the aggregate of N identical molecules is then:

$$H = \sum_{i=1}^{N} h_i + \sum_{j>i}^{N} V_{ij} \tag{1}$$

Here, h_i is the free-molecule Hamiltonian whose ground- and excited-state wave functions are φ_i and φ_i^*, respectively, and V_{ij} represents the intermolecular interaction potential.

In zeroth-order, the exciton states Ψ_k of the system can be written as linear combinations of N locally singly-excited states following a Davidov-like formalism of excitation transfer [5, 7, 8].

$$\Psi_k = \sum_{i=1}^{N} C_{ki} \Phi_i \qquad k = 1, 2, \ldots, N \tag{2}$$

where

$$\Phi_i = \varphi_i^* \prod_{j \neq i}^{N} \varphi_j \qquad i = 1, 2, \ldots, N$$

In the present work we have neglected electron exchange between molecules. The lowest state eigenvalue λ_1 and its corresponding state function Ψ_1 is then found solving the secular equation:

$$|H_{ij} - \lambda S_{ij}| = 0 \tag{3}$$

where $S_{ij} = \delta_{ij}$ due to orthogonality of the functions Φ_i. For each molecule we write its electronic energy in terms of the local equilibrium position displacement Q_i as:

$$\langle \varphi_i | h_i | \varphi_i \rangle = w + \tfrac{1}{2} k (Q_i - Q_0)^2 = w + e_i \tag{4a}$$

and

$$\langle \varphi_i^* | h_i | \varphi_i^* \rangle = w^* + \tfrac{1}{2} k^* (Q_i - Q_0^*)^2 = w_i^* + e_i^* \tag{4b}$$

here w and w^* are the ground- and excited-state free-molecule electronic energies respectively, evaluated at the corresponding equilibrium positions.

The following definitions must also be introduced:

$$\begin{aligned} \langle \varphi_i \varphi_j | V_{ij} | \varphi_i \varphi_j \rangle &= V \\ \langle \varphi_i^* \varphi_j | V_{ij} | \varphi_i^* \varphi_j \rangle &= V^* \end{aligned} \tag{5}$$

which are the coulombic interactions between unexcited molecules and between unexcited-excited molecules respectively, and also:

$$\langle \varphi_i^* \varphi_j | V_{ij} | \varphi_i \varphi_j^* \rangle = U' \tag{6}$$

the pseudo-coulombic interaction between transition-charge densities [5, 6].

With the help of these definitions, the matrix elements of Eq. (3) are found to be:

$$H_{ii} = \langle \Phi_i | H | \Phi_i \rangle = w^* + e_i^* + \sum_{j \neq i}^{N} (w + e_j) + (N-1)V^* + \tfrac{1}{2}(N-1)(N-2)V \tag{7}$$

and

$$H_{ij} = \langle \Phi_i | H | \Phi_j \rangle = U' \tag{8}$$

here, V and V^* represent average values of coulombic pair interactions within the whole aggregate. In an aggregate of identical molecules, the electronic energy at the equilibrium position is the same for all of them, then without loss of generality, it is found convenient for solving Eq. (3), to measure energies relative to the constant value:

$$w^* + (N-1)w + (N-1)V^* + \tfrac{1}{2}(N-1)(N-2)V$$

in order to simplify the matrix elements. We simultaneously change to dimensionless variables by measuring energies in units of $\frac{1}{4}(k+k^*)(Q_0-Q_0^*)^2$ and thus we can rewrite Eqs. (7) and (8) in dimensionless form. These become now:

$$H_{ii}=2\left\{(1-K)q_i^2-\frac{2q_i(1-K\varrho)}{(\varrho-1)}+\frac{2(1-K\varrho^2)}{(\varrho-1)^2}\right\}$$
$$+\sum_{j=1}^{N}\frac{2K}{(1+K)}\left\{q_j^2-\frac{2\varrho q_j}{(\varrho-1)}+\frac{\varrho^2}{(\varrho-1)^2}\right\} \tag{9}$$

and

$$H_{ij}=\frac{4U'}{(k+k^*)(Q_0-Q_0^*)^2}=U$$

In these equations we have introduced two dimensionless parameters:

$$\varrho=\frac{Q_0}{Q_0^*} \quad \text{and} \quad K=\frac{k}{k^*}$$

which measure the degree of distribution of the potential surfaces (i.e. the changes in equilibrium position and force constant) along the coordinate Q_i of the ground- compared to the excited-state of a free molecule. We also have introduced the dimensionless distortion coordinate:

$$q_k=\frac{Q_k}{(Q_0-Q_0^*)}$$

3. Results

In principle, Eq. (3), with its matrix elements given by Eq. (9), can be solved analytically to yield vibrational potential functions, defined in the space spanned by the N coordinates $\{q_i\}$, in which the effect, in first-order, of intermolecular vibronic coupling on the energy localization and transfer can be interpreted by analysing the changes in such potentials. Analytical surfaces obtained in this way have been pictured in three dimensions for the case of a small molecular aggregate with five molecules [8] but for more bulky arrangements, Eq. (3) must be solved numerically once the input variables q_i $(i=1,2,\ldots,N)$ have been defined in a specific configuration (i.e. location of the excitation in a specific molecule within the aggregate). Nevertheless, it is not simple to make a drawing of these surfaces and extract conclusions due to the high number of variables. We will illustrate this analytical procedure for small flat closed-packed arrangement of spherical molecules, where we can take advantage of the inherent C_6 symmetry.

In the molecular aggregate of Fig. 1, consisting of 19 identical molecules in closed packing arrangement, we take the central portion, that is, the central molecule (labelled 1) and the first surrounding layer of molecules (labelled 2–7) and treat this portion as a small 7-molecule aggregate. For this aggregate, analytical solutions for the lowest eigenvalue in Eq. (3) have been found [11] provided that the coordinate Q_i, representing the distortion in equilibrium position, is itself totally symmetric i.e. like the molecular breathing motion, for we can represent the collective vibrational motions of the whole aggregate then in C_6 symmetry. The set of seven vibrations $\{Q_i\}$ (or $\{q_i\}$) in this symmetry gives

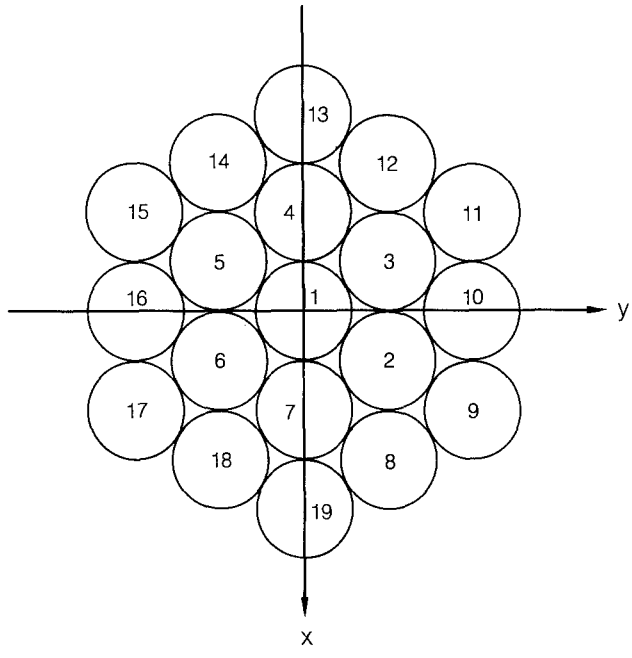

Fig. 1. The relative position and numbering of molecules in a 19-molecule flat aggregate in closed-packing arrangement

rise to $A + B + E_1 + E_2$ symmetry species whose associated collective motions $\{\theta_i\}$ are:

$$\begin{aligned}
A &\quad \begin{cases} \theta_1 = q_1 + (q_2 + q_3 + q_4 + q_5 + q_6 + q_7) \\ \theta_2 = -q_1 + (q_2 + q_3 + q_4 + q_5 + q_6 + q_7) \end{cases} \\
B &\quad \{\theta_3 = -q_2 + q_3 - q_4 + q_5 - q_6 + q_7 \\
E_1 &\quad \begin{cases} \theta_4 = q_2 + 2q_3 + q_4 - q_5 - 2q_6 - q_7 \\ \theta_5 = 2q_2 + q_3 - q_4 - 2q_5 - q_6 + q_7 \end{cases} \\
E_2 &\quad \begin{cases} \theta_6 = 2q_2 - q_3 - q_4 + 2q_5 - q_6 - q_7 \\ \theta_7 = -q_2 + 2q_3 - q_4 - q_5 + 2q_6 - q_7 \end{cases}
\end{aligned} \tag{10}$$

and the inverse transformation:

$$\begin{aligned}
q_1 &= \tfrac{1}{12}(\theta_1 - \theta_2) \\
q_2 &= \tfrac{1}{12}(\theta_1 + \theta_2 - 2\theta_3 + 2\theta_5 + 2\theta_6) \\
q_3 &= \tfrac{1}{12}(\theta_1 + \theta_2 + 2\theta_3 + 2\theta_4 + 2\theta_7) \\
q_4 &= \tfrac{1}{12}(\theta_1 + \theta_2 - 2\theta_3 + 2\theta_4 - 2\theta_5 - 2\theta_6 - 2\theta_7) \\
q_5 &= \tfrac{1}{12}(\theta_1 + \theta_2 + 2\theta_3 - 2\theta_5 + 2\theta_6) \\
q_6 &= \tfrac{1}{12}(\theta_1 + \theta_2 - 2\theta_3 - 2\theta_4 + 2\theta_7) \\
q_7 &= \tfrac{1}{12}(\theta_1 + \theta_2 + 2\theta_3 - 2\theta_4 + 2\theta_5 - 2\theta_6 - 2\theta_7)
\end{aligned} \tag{11}$$

With the help of Eq. (11), all diagonal elements H_{ii} in Eq. (9) can be rewritten in terms of the set of collective vibrations $\{\theta_i\}$, giving rise to long expressions which are not given here. The simplest analysis one can do is to take the limit $U \to 0$. In this situation, the eigenvalues are clearly $\lambda_k = H_{kk}$ $(k = 1, 2, \ldots, 7)$

Table 1. Lowest eigenvalue λ of a 7-molecule aggregate in the limit $U = 0.0$ or $\lambda_k = H_{kk}$. Here $A = (6+\varrho)/(1-\varrho)$, $B = (6-\varrho)/(1-\varrho)$, $C = (4+\varrho)/(1-\varrho)$

Eigvl.	θ_1	θ_2	θ_3	θ_4	θ_5	θ_6	θ_7
λ_1	A	B	0	0	0	0	0
λ_2	A	C	1	−1	−2	−2	1
λ_3	A	C	−1	−2	−1	1	−2
λ_4	A	C	1	−1	1	1	1
λ_5	A	C	−1	1	2	−2	2
λ_6	A	C	1	2	1	1	1
λ_7	A	C	−1	1	−1	1	−1

and for specific values of the variables $\{\theta_i\}$, one of these eigenvalues in turn, corresponds to the lowest eigenvalue. Thus, we search for the set of collective vibrations $\{\theta_i\}_k$ that minimize λ_k, that is:

$$\frac{\partial H_{kk}}{\partial \theta_j} = 0 \quad \text{for all } j \neq 1, \text{ where } k = 1, 2, \ldots, 7$$

We have excluded coordinate θ_1 because if one of the molecules is to be excited, then its value is always $\theta_1 = (6+\varrho)/(1-\varrho)$ in each one of all minima.

The values of $\{\theta_i\}_k$ that give minimum values for $\lambda_k = H_{kk}$ are summarized in Table 1. With the aid of this table and the definitions of Eqs. (11), it is readily seen that for the minimum $\lambda_1 = H_{11}$ we have:

$$q_1 = \frac{\varrho}{(1-\varrho)} = \frac{Q_0^*}{(Q_0 - Q_0^*)} \quad \text{and that} \quad q_2 = q_3 = \cdots = q_7 = \frac{1}{(1-\varrho)} = \frac{Q_0}{(Q_0 - Q_0^*)}$$

similarly, for the minimum $\lambda_2 = H_{22}$, we find instead:

$$q_2 = \frac{\varrho}{(1-\varrho)} = \frac{Q_0^*}{(Q_0 - Q_0^*)} \quad \text{and that} \quad q_1 = q_3 = \cdots = q_7 = \frac{1}{(1-\varrho)} = \frac{Q_0}{(Q_0 - Q_0^*)}$$

and so on.

These eigenvalues, computed at the minima, correspond to values at specific points of the potential hypersurface for the collective vibrations of the aggregate in the space of N coordinates $\{\theta_i\}$. In absence of resonance interaction U, all these eigenvalues have of course the same magnitude, as can be seen from Eq. (7); this is not necessarily so when we allow the molecules to interact and, furthermore, the values $\{\theta_i\}$ at which the minima occur suffer considerable changes as it will be seen later. The important fact is that in the space spanned by $\{\theta_i\}$, the potential energy hypersurface shows N minima, correspondingly with the excitation being localized at a specific molecule.

We focus our attention now on certain collective vibrations which "promote" the excitation transfer among molecules. These modes are θ_2 and θ_3 (see Eqs. (10)).

We will take as an example the mode θ_2. From Table 1 we see that the eigenvalue λ_1 at its minimum value means $\theta_2 = (6-\varrho)/(1-\varrho)$, that is $Q_1 = Q_0^*$ or that the excitation is at the center molecule, whereas for $\lambda_{i\neq 1}$ at their respective minimum means $\theta_2 = (4+\varrho)/(1-\varrho)$, that is to say $Q_i = Q_0^*$ or that the excitation is now located at one of the external molecules. Along coordinate

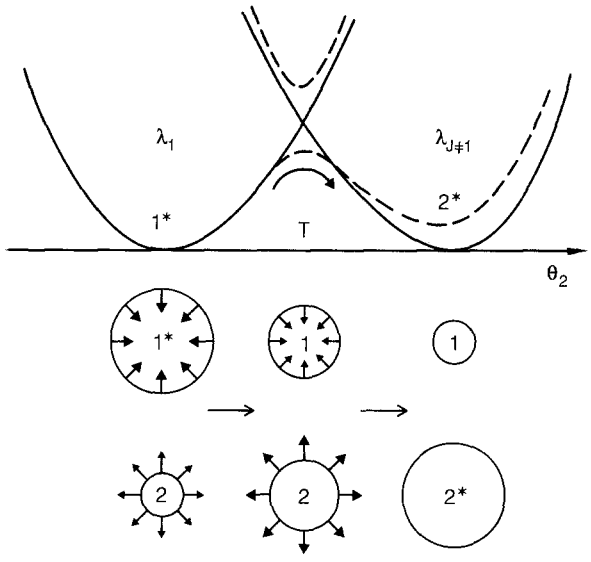

Fig. 2. Energy profile along the out-of-phase collective vibration θ_2 (the limit $U \approx 0$ (*solid line*) and $U > 0$ (*dotted line*)) and a schematic drawing of the expansion-contraction stages of molecules "1" and "2" (it is assumed that $Q_0^* > Q_0$)

θ_2 therefore we can draw a potential curve with two minima which describe the two above situations and which are shown in Fig. 2 for the limit $U \approx 0$. For zero intermolecular interaction these curves are two adjacent oscillators. There will be an energy barrier between the two minima at the crossing point which will decrease as we allow the intermolecular interaction to increase.

Now consider that we look into the transfer of excitation between molecules "1" and "2" and that we assume that for the excited molecule $Q_0^* > Q_0$, that is, in this breathing motion the molecule contracts itself after giving off the excitation.

In the collective mode θ_2, molecules "1" and "2" vibrate out-of-phase, as it is sketched in Fig. 2. In this figure, we show schematically the transfer of excitation to molecule "2" from molecule "1" through the passage over the energy barrier, if vibrational distortions are big enough or by tunnelling, which also might be of importance for low vibrational levels. In any case, we start out in the left well of Fig. 2 and see how the system moves toward the right. There is a "transition point" (marked T in Fig. 2) where molecule "1" in its process of contraction and molecule "2" in its process of expansion both would have reached their respective turning points if they were at the top of the barrier, but instead of reversing their vibrations, they continue contracting and expanding respectively and the system eventually falls in in the potential well at the right, which describes the potential energy of an outer molecule bearing the excitation (in this case molecule "2"). The transfer of excitation is thus accomplished by a smooth crossing of the energy barrier accompanied also by a smooth transfer of vibrational distortion energy.

The flow of excitation among the external molecules is accomplished with the help of the "promoting" collective mode θ_3. Again, if we sketch potential curves along this coordinate, we find a two-well system with its extrema located at $\theta_3 = -1$ and $\theta_3 = +1$ respectively in a fashion very similar to Fig. 2. In this case, however, the left well corresponds to odd-numbered eigenvalues (excitation

localized in odd-numbered molecules) and the well at the right to even-numbered eigenvalues (excitation in even-numbered molecules). We follow a similar line of reasoning to that given above for θ_2 as a "promoting" mode, but now is readily seen from Table 1 that the transfer always occurs between an odd-numbered molecule and an even-numbered molecule and vice versa.

When the intermolecular interaction U increases, it is found that λ_1 is lowered with respect $\lambda_{j\neq 1}$ (see Fig. 2) and also there is a lowering of the barrier, which for large interactions become itself a minimum. This last situation describes the excitation delocalization between pairs of molecules.

For more bulky molecular aggregates, such as the 19-molecule of Fig. 1, it is still possible to make few simplifications if we grant spherical symmetry to the vibration Q_i and define "promoting" collective modes. Nevertheless, we have studied the more general case of the 19-molecule aggregate of Fig. 1 in closed-packed arrangement where the symmetry of Q_i has not been taken into account. Here Eq. (3) was solved numerically after defining the input variables q_i ($i = 1, 2, \ldots, 19$).

To carry out computations, we assumed that bonding in an excited molecule is weaker compared to bonding in an unexcited one. We arbitrarily assumed a 10 percent enhancement of the equilibrium position and a 5 percent weakening of the force constant in the excited state and therefore the parameters ϱ and K were given the values 0.90 and 1.05, respectively. These values are likely though to represent a real situation. We tested, nevertheless, the effect of varying these parameters on the eigenvalues of Eq. (3) but these turned out to be quite insensitive to both ϱ and K and therefore their arbitrary choice does not have an effect on the overall qualitative conclusions drawn in the present work.

Calculations were made for several locations of a single excitation among the molecules of an aggregate consisting of 19 identical molecules (see Fig. 1) in planar arrangement. We assumed spherical shape for drawing purposes although only their relative location is important. There is also no imposed restrictions on the symmetry of the coordinate Q_i. We solved then Eq. (3) by standard diagonalization methods and concentrated only on the lowest eigenvalue λ_1 and its respective eigenfunction Ψ_1 computed for configurations consisting of either, the electronic excitation localized in the jth molecule, a state that we denote $\Psi_1(j)$ or $(j)^*$, or, the excitation being "shared" (i.e. delocalized) among a group of neighbor molecules, say the jth and the kth, a state that we denote $\Psi_1(j\text{–}k)$ or $(j\text{–}k)^*$.

In Figs. 3, 4, and 5 we show energy surfaces (that is λ_1) as a function of the relative location of the excitation in the molecular aggregate for the weak-coupling case ($U \approx 0$) in Fig. 1, the strong-coupling case ($U \geqslant 1.0$) in Fig. 4 and an intermediate case in Fig. 5. In all these figures we show only the positive quadrant of Fig. 1. The rest of the aggregate produces identical surface drawings. The set of axes is the same as in Fig. 1 and we have also included the molecule label for clearness.

In these figures, the highest peaks correspond to $(i\text{–}j\text{–}k)^*$ configurations or delocalization among three neighbor molecules but are actually much higher than as they appear there (see Table 2) and have been cut-down for drawing purposes; besides, only $(i)^*$, $(i\text{–}j)^*$ and $(1\text{–}j\text{–}k)^*$ configurations were calculated and therefore Figs. 3 and 4 and also 5 are smoothened surfaces drawn using splines technics.

Figures 3, 4, and 5 need also further explanation. In these graphs we have plotted the energy of the lowest eigenvalue vs. a specific configuration (i.e.

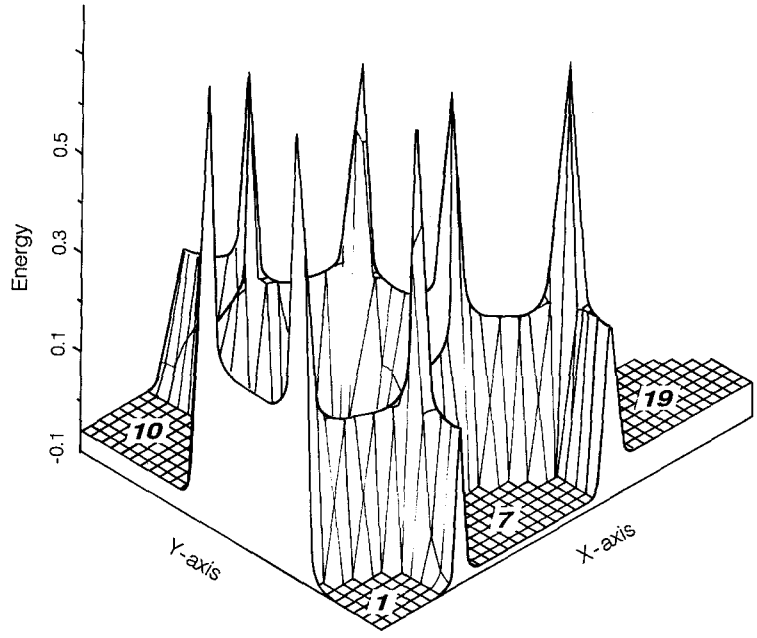

Fig. 3. Computer drawing for the weak-coupling case ($U = 0.2$) of the state energy surface for configurations $(i)^*$, $(i\text{–}j)^*$ and $(i\text{–}j\text{–}k)^*$. (Energy in units of $\frac{1}{4}(k + k^*)(Q_0 - Q_0^*)^2$). For configurations $(i)^*$, the energy is constant within the boundary of molecule i, all other values correspond to situations of "sharing" of excitation

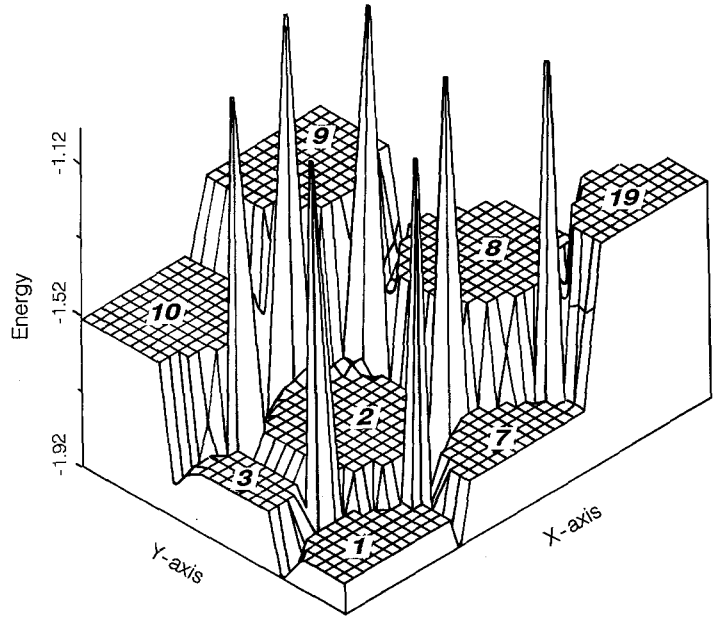

Fig. 4. Computer drawing of the strong-coupled case ($U = 1.2$) of the state energy surface for configurations $(i)^*$, $(i\text{–}j)^*$ and $(i\text{–}j\text{–}k)^*$. (Energy in units of $\frac{1}{2}(k + k^*)(Q_0 - Q_0^*)^2$)

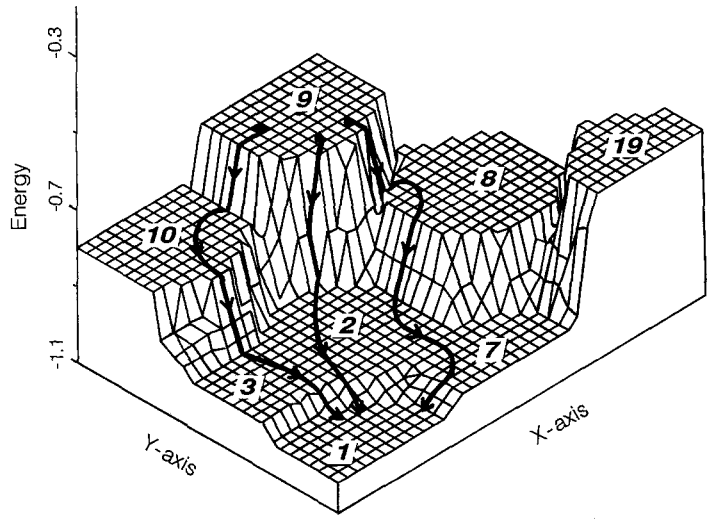

Fig. 5. The energy state surface for the intermediate-coupling case ($U = 0.8$). The peaks $(i-j-k)^*$ have been removed and some favorable trajectories for inward excitation shown

Table 2. Lowest eigenvalue λ_1 (in units of $\frac{1}{4}(k+k^*)(Q_0 - Q_0^*)^2$) for a 19-molecule aggregate. The strong-($U = 1.2$), intermediate-($U = 0.8$) and weak-($U = 0.2$) coupling case

Config.	Weak coupling	Intermediate coupling	Strong coupling
(1)*	−0.0993	−0.0186	−1.8355
(2)*	−0.0982	−0.9777	−1.7887
(8)*	−0.0694	−0.7981	−1.5268
(19)*	−0.0532	−0.6658	−1.3450
(1–2)*	+0.2174	−1.0004	−1.9181
(2–7)*	+0.2181	−0.9759	−1.8679
(2–9)*	+0.2153	−0.8532	−1.7413
(2–8)*	+0.2382	−0.9071	−1.8025
(8–19)*	+0.2525	−0.8208	−1.7055
(1–2–7)*	+22.397	+21.080	+20.190
(2–7–8)*	+22.363	+20.950	+20.150
(2–8–9)*	+22.354	+20.930	+20.150
(8–9–19)*	+22.253	+20.870	+20.070
(1–2–5)*	+22.396	+21.050	+20.180

location of the excitation) and therefore the X and Y axes are given only for reference purposes; that is to specify the boundary regions between molecules and regions of the XY plane occupied by the molecules and do not represent coordinates of molecular distortions.

While the excitation is localized in a specific molecule, the eigenvalue remains the same within the boundaries of that molecule, and that fact is

Table 3. The coefficients $C_{1,m}$ of the lowest eigenstate $\Psi_1(ijk)$ (see Eq. 2) corresponding to the configuration $(i-j-k)^*$ for the strong-($U = 1.2$) and weak-($U = 0.2$) coupling case

	$\Psi_1(1)$		$\Psi_1(1, 2)$		$\Psi_1(1, 2, 3)$	
Coeff.	Weak	Strong	Weak	Strong	Weak	Strong
$C_{1,1}$	1.000	1.000	0.995	1.000	0.000	0.295
$C_{1,2}$	−0.045	−0.255	1.000	−0.818	0.010	−0.090
$C_{1,3}$	−0.045	−0.255	−0.198	−0.060	−0.010	−0.090
$C_{1,4}$	−0.045	−0.255	−0.079	−0.441	0.668	−0.521
$C_{1,5}$	−0.045	−0.255	−0.092	−0.194	−1.000	−0.308
$C_{1,6}$	−0.045	−0.255	−0.079	−0.441	1.000	−0.310
$C_{1,7}$	−0.045	−0.255	−0.198	−0.060	−0.671	−0.520
$C_{1,8}$	0.004	0.180	−0.077	0.370	0.274	0.855
$C_{1,9}$	0.002	−0.033	−0.088	0.027	−0.133	−0.659
$C_{1,10}$	0.004	0.180	−0.077	0.370	0.002	0.683
$C_{1,11}$	0.002	−0.033	0.026	−0.201	0.128	−0.660
$C_{1,12}$	0.004	0.180	0.026	0.260	−0.269	0.856
$C_{1,13}$	0.002	−0.033	0.003	−0.035	−0.205	−0.608
$C_{1,14}$	0.004	0.180	0.017	0.282	0.044	0.998
$C_{1,15}$	0.002	−0.033	0.006	−0.130	0.442	−0.757
$C_{1,16}$	0.004	0.180	0.017	0.282	0.001	0.971
$C_{1,17}$	0.002	−0.033	0.003	−0.035	−0.446	−0.757
$C_{1,18}$	0.004	0.180	0.026	0.260	−0.040	1.000
$C_{1,19}$	0.002	−0.033	0.026	−0.202	0.203	−0.608

represented in Figs. 3, 4, and 5 by a flat surface labelled correspondingly. The actual vibronic hypersurface cannot be represented in this manner.

For the configuration $(1)^*$, that is, we have computed Eqs. (9) with $q_1 = 1/(\varrho - 1)$ and $q_{j\neq 1} = \varrho/(\varrho - 1)$ which in turn means $Q_1 = Q_0^*$ and $Q_{j\neq 1} = Q_0$. The resulting eigenfunction $\Psi_1(1)$ is predictably highly localized in molecule "1" for weak interaction ($U \cong 0$) as is shown in Table 3 but tends to delocalize among neighbor molecules with increasing interaction U. The corresponding eigenvalues appear in Table 2 for both the weak- and strong-coupling case.

The wave function for a configuration such as $(1-2)^*$, where the excitation is delocalized between two adjacent molecules, is also shown in Table 3. Here we have computed the matrix elements of Eqs. (9) with:

$$q_1 = q_2 = \frac{1+\varrho}{2(\varrho-1)} \quad \text{and} \quad q_{j\neq 1,2} = \frac{\varrho}{(\varrho-1)}$$

which in turn means:

$$Q_1 = Q_2 = \tfrac{1}{2}(Q_0 + Q_0^*) \quad \text{and} \quad Q_{j\neq 1,2} = Q_0.$$

The outcoming wave function $\Psi_1(1, 2)$ shows delocalization mainly between molecules "1" and "2" for weak interaction but exhibits increasing delocalization among the rest of the molecules of the aggregate as the interaction increases. These results are summarized in Tables 2 and 3. There we also show the wave

function for the configuration (1–2–3)* where three molecules "share" the excitation. In this case, the matrix elements of Eqs. (9) were computed with:

$$q_1 = q_2 = q_3 = \frac{1+\varrho}{3(\varrho-1)} \quad \text{and} \quad q_{j\neq 1,2,3} = \frac{\varrho}{(\varrho-1)}.$$

The wave function now turned out to be entirely delocalized among the rest of the molecules of the aggregate for both the weak- and strong-coupled limits. The energy of such a configuration is very high and is shown in Figs. 3 and 4 and also in Table 2.

We return now to Figs. 3 and 4. From the shape of the potential energy functions, we see that, for the weak-coupling case, the excitation tends to be localized in a single molecule and that the central molecule is associated with the lowest energy configuration, a result that might seem obvious if one simply counts the number of interactions with surrounding molecules. Since in this model we are considering only nearest neighbor interactions, if that were true, then the energy for the (1)* type configuration should be equal to that of (2)* configuration, but they are not, as can be seen in Table 2, and this difference increases with increasing interaction.

For the strong-coupling limit, delocalized configurations of $(i-j)$* type are lower energy in energy compared to the (i)* type and again their relative energy increases as the molecules involved are located farther apart from the center of the aggregate.

This is clearly a sort of "mirror image" of the features of the weak-coupling limit and therefore there should be an intermediate value of U for which the potential energy function increases monotonically, along certain "paths", with the distance from the central molecule. We have found that for a value of $U \cong 0.80$ the energy barrier for the transfer of excitation between pairs of adjacent molecules disappear and that the excitation is almost free to flow among the molecules and preferably toward the central molecule. These results are shown in Fig. 5. In this figure we have suppressed the peaks corresponding to $(i-j-k)$* configurations in order to get a clearer view of possible "paths" for energy flowing in the aggregate.

We see in Fig. 5 that, in a "radial path" (i.e. molec. 9 → molec. 2 → molec. 1), the excitation will readily flow toward the central molecule following a favorable energy gradient with no barrier or "trapping" energy wells, while there are shallow delocalized trapping wells, between exterior molecular pairs, for any other trajectory (for example, in paths such as molec. 9 → 8 → 2 → 7 → 1 there is delocalized trapping between molecules 9 and 8 in Fig. 5). The flowing of excitation in circular paths becomes almost free near the center of the aggregate for this optimum value of U while there is some delocalized trapping with increasing distance from the center of the aggregate.

Within the framework of the present model, the relative orientation of the molecular dipoles (i.e. the sign of U) has no substantial effect on the state energies since a square dependence on U is expected in the diagonalization process and thus, the qualitative conclusions drawn in the present work do not change appreciably. Inclusion of non-nearest neighbor interactions is of even less importance.

Acknowledgements. The author J.R.L. is indebted to the Catholic University of America for a sabbatical semester where part of this work was done and to D.T.I. University of Chile (Project No. Q2861) for financial support.

References

1. Emerson R, Arnold W (1932) J Gen Physiol 15:391
2. Franck J, Teller E (1938) J Chem Phys 6:861
3. Paillotin G (1972) J Theor Biol 36:223
4. Seely GR (1973) J Theor Biol 40:173; (1973) ibid 40:189
5. Letelier JR, Chiu YN (1977) Chem Phys Letters 52:359
6. Föster T (1965) in: Modern quantum chemistry, Part III, Academic Press, N.Y.; Föster T (1965) Bull No 18, Div. of Biology and Medicine, U.S. Atomic Energy Commission
7. Davidov AS (1962) Theory of molecular excitons. McGraw-Hill, N.Y.
8. Varas RE, Letelier JR (1990) Chem Phys Letters 170:253
9. Kenre VM, Knox RS (1974) Phys Rev Letters 33:803
10. Knox RS (1977) in: Barber J (ed) Topics in photosynthesis, Vol 2, Elsevier, N.Y.
11. Varas RE (1988) Thesis submitted to Facultad de Ciencias Físicas y Matemáticas, Universidad de Chile